A Low Cost Outdoor Air Pollution Monitoring Device with Power Controlled Built-In PM Sensor

Payali Das, Sushmita Ghosh, Shouri Chatterjee, and Swades De

***Abstract*— Recent advances in wireless communication technology and the Internet of Things (IoT) have provided an opportunity for mass deployment of low cost sensor nodes to measure air pollution in real-time over a large geographical area. This article presents the design of a low cost, innovative Air Pollution Monitoring Device (APMD) along with the evaluation of its advanced features. An on-board Particulate Matter (PM) sensor is designed to measure $PM_{2.5}$ and PM_{10}. APMD additionally has electrochemical sensors to measure carbon monoxide, sulphur dioxide, nitrogen dioxide, ozone, besides temperature and humidity sensors. The node is equipped with a solar energy harvesting unit and a rechargeable battery as a backup to power up the module. By utilizing an on-board GPS subsystem, APMD packs all these gathered air quality data in a frame with physical location, time, and date, and sends them to a cloud server. The node can communicate through WiFi and NB-IoT connectivity. For validating the quality of sensing, the developed APMD was co-located with an accurate reference sensor node and a series of field data were collected over seven days. In a fully ON state, the on-board PM sensor saves up to 94% energy while maintaining root mean square error (RMSE) of 0.58 for $PM_{2.5}$ and 2.5 for PM_{10}. A power control mechanism is also applied on the PM sensor to control the speed of the fan by applying a pulse width modulated (PWM) signal at the switch connected to the power supply of fan. At 100 ms switching period with 30% duty cycle, the on-board PM sensor is 97% energy efficient compared to the commercial sensor, while maintaining sensing error (RMSE) as low as 0.7 for $PM_{2.5}$ and 2.7 for PM_{10}. Our outdoor deployment studies demonstrate that the designed APMD is 90.8% more power efficient than the reference setup with significantly higher coverage range, while maintaining an acceptable range of sensing error.**

***Index Terms*— Air pollution monitoring device, temporal correlation, in-built PM sensor, optimum sampling interval, ambient energy harvesting**

I. Introduction

Air pollution in urban areas has many harmful effects on humans and the environment. Air contamination is mainly caused by vehicles and industries which cause various respiratory diseases, such as asthma and sinusitis. The health effects of air pollution are serious; one-third of deaths from stroke, lung cancer, and heart disease are due to air pollution. Microscopic Particulate Matters (PMs) in the air can slip past human body defenses, penetrating deep into our respiratory and circulatory system, damaging our lungs, heart, and brain. World Health Organization (WHO) air quality model confirms that 92% of the world's population lives in places where air quality levels exceed WHO prescribed safety limits. Nearly 90% of air-pollution-related deaths occur in low- and middle-income countries, with nearly 2 out of 3 occurring in WHO's South-East Asia and Western Pacific regions [1]. Hence pollution localization and large scale sensing are needed which requires low cost and energy sustainable pollution monitoring nodes to be deployed on a large scale; sparsely deployed monitors are unable to do this job effectively.

The steady advancement of Internet of Things (IoT) technology, sensor technology, and information communication technology (ICT) has enabled us to monitor the environment in which people work and live, at any time [2]. The work in [3] reported multiple connectivity based environment monitoring system. Here a sensing system using sensor arrays was developed to monitor indoor as well as outdoor environments. However, these systems are costly and may not be suitable for large-scale deployment.

More than 21.5 billion interconnected devices are currently available in the world which is expected to grow by 500 billion by 2030 [4]. Newer solutions of wireless network technologies are therefore required to support the fast development and adoption of IoT. This is also essential due to the specific requirements and characteristics of IoT devices such as low power consumption, long-range, low cost, and security. The storage and processing capabilities are also restricted by the resources available, which are often very constrained due to limitations of size, energy, and computational capability. Thus, context-specific affordable implementation of IoT is of pertinent importance [5]. To this end, narrow band IoT (NB-IoT) is considered a promising wireless communications technology for IoT because of its super coverage extension, a massive number of connections, and low power requirement. In Low Power Wide Area (LPWA) networks, NB-IoT connectivity is widely applicable in application scenarios, such as environment monitoring, smart metering, smart parking, smart home, smart tracking, and e-health [6].

Despite the evolution of low power communication capabilities, environmental pollution sensing IoT devices are inherently energy hungry. This is because the sensing activity

Payali Das, Sushmita Ghosh, Shouri Chatterjee, and Swades De are with the Department of Electrical Engineering and UQ-IITD Academy, Indian Institute of Technology Delhi, New Delhi, India (e-mail: Payali.Das@ee.iitd.ac.in, qiz198439@uqidar.iitd.ac.in, swadesd@ee.iitd.ac.in, shouri@ee.iitd.ac.in).

itself involves various electrical and electrochemical activities. Therefore, for scalability, cost, and convenience, developing more energy-efficient sensing is of significant interest in the research community. An associated concern from open hand convenience is the reliability of sensed data using low cost miniature IoT sensor nodes and the possibility of automated self correction of the sensed data accuracy.

A. Literature Survey

Quite a few works have been reported in the literature on developing air pollution sensing devices to monitor the pollutants in the environment. In [3], an indoor environment pollution gas monitoring system with CO and CO_2, including a sensor array was implemented in hardware using a DSP board for real-time processing. Another study in [2] developed an Indoor Air Quality Device (IAQD) by using advanced IoT techniques. Five parameters could be detected by IAQD: humidity, temperature, formaldehyde, CO_2, and $PM_{2.5}$. To make the system handy with different applications, IAQD was designed with multiple communication interfaces, including LoRa, NB-IoT, RS485, and WiFi. Zigbee based wireless indoor air quality monitoring system was developed in [7], [8]. However, as the sensors use resistive heating, low battery lifetime is one of the major drawbacks of the system. The sensor module prototype was designed with a WaspMote from Libelium Communications. A low-power air quality monitoring board CitiSense was presented in [9], where low cost wearable sensor nodes are used along with smart phones to monitor the environment. CO, NO_2, O_3, temperature, humidity, and barometric pressure are sensed and the data is communicated via Bluetooth. LoRaWAN based air pollution monitoring systems are developed in [10]–[12]. However, these prototypes are not energy efficient and have complex system architecture. The design of a metropolitan air pollution monitoring system Haze Watch is described in [13]. This battery powered node utilized Bluetooth technology for communicating data to a cloud server. The measured values of CO, NO_2, and O_3 were then accessible through a mobile application. In the project MAQUMON [14], a portable wireless sensor node was developed for measuring O_3, NO_2, and CO. These autonomous units have on-board GPS and flash for storage and use GPS for communication purposes. In [15] an air quality monitoring system is described. However, this Bluetooth based sensor box has a low communication range, and no validation of data accuracy is performed. A GPRS based sensor system is described in [16]. This mobile data acquisition unit measures CO, NO_2, and SO_2 from the ambient environment. The pollution server is interfaced with Google maps to display real-time pollution values. A wireless sensing system was designed in [17] that uploads the gathered sensor data to the server using a mobile network. However, any field testing or validation results were not reported.

B. Research Gap and Motivation

Due to the technological limitation of pollution source localization, enforcement of emission norms is still not settled. Network-capable low cost and low energy consuming pollution monitoring devices are needed for pollution localization. Scientific ways of air pollution monitoring and identification of the causes of air pollution are very limited in developing countries. For example, in India, Delhi region has only 36 Pollution Measuring Stations and cannot scale further [18].

In [19], a mobile air pollution monitoring framework was proposed. However, it did not present any test-bed setup. It considered WiFi based connectivity which is power hungry. In [10], low cost sensor development was reported based on LoRa connectivity. This approach may not work well in a massive deployment scenario. The maximum coupling loss (MCL) is the limit value of service delivery which in turn defines the range of service [20]. The uplink MCL in LoRa is 165 dB which provides up to 15 km coverage range, whereas in NB-IoT it is up to 169 dB which ensures up to 35 km coverage range [21]. Therefore, for better communication energy efficiency in our design we have chosen NB-IoT as the preferred communication technology. The work reported in [2], primarily focused its study on indoor environments.

Requirement of air pollution monitoring includes massive deployment of sensor nodes for pollution source localization while accounting for uninterrupted operation. Battery powered systems can not serve this goal efficiently. Energy harvesting devices are self-sustainable and can be deployed easily at remote locations. This is in contrast with the deployment of battery-operated devices which is not scalable due to the need for occasional battery replacement. Majority of previous works had WiFi or Bluetooth as the communication interface, which has low range and consumes high energy for communication. This drawback makes it hard to deploy the sensor nodes outdoor on a massive scale. *To address the prevailing issues in pollution localization and large scale monitoring, this paper reports design of a low energy consuming air pollution monitoring device, including PM sensor, NB-IoT radio module, a monitoring/processing unit, and solar energy harvesting capability.* In this work, outdoor pollution monitoring is considered as the primary application.

According to [22], the PM sensor consumes the highest energy among all the air pollution monitoring sensors, which reduces the battery lifetime. *To devise a self-sustainable APMD, a low energy consuming PM sensor is developed which uses LED light scattering principle in contrast to the laser light scattering principle that the commercial PM sensors use. To further optimize the energy consumption of the on-board PM sensor, this paper also proposes a power control mechanism by switching the power supply of the fan.* The aim is to make the device self-sustainable while maintaining the sensing quality within the acceptable range.

C. Contribution and Significance

The key contributions and significance are as follows:

1) We report the design of a low cost, energy-efficient multi-sensing module for air pollution monitoring, called advanced pollution monitoring device (APMD), which is equipped for monitoring eight environmental parameters, namely, NO_2, SO_2, CO, O_3, $PM_{2.5}$, PM_{10},

temperature, and humidity, along with alternative radio interfaces, NB-IoT or WiFi, for communication.

2) PM sensor module consumes the highest power; it is replaced by our innovative on-board PM sensor that saves up to 94% energy compared to the traditional one.
3) A power control mechanism is also developed to control the power of the on-board PM sensor by switching the power supply of the fan. Applying a PWM signal of 100 ms with 30% duty cycle at the switch, the designed on-board PM sensor saves 97% energy compared to the traditional PM sensor, while the sensing error of RMSE $= 0.7$ for $PM_{2.5}$ and RMSE $= 2.7$ for PM_{10}.
4) The designed APMD is 90.8% and 98.3% more power efficient compared to a reference prototype and commercially available competitive devices, respectively.
5) With its very low energy consumption footprint, the device is capable to operate using solar power, thus achieving energy sustainable/green sensing solution.

Organization: The system design and implementation strategy is presented in Section II, followed by brief descriptions of the different basic modules used in hardware implementation in Section III. Section IV describes the design of the on-board PM sensor along with its power control mechanism. The prototype design is presented in Section V, followed by results and conclusion in Sections VI and VII, respectively.

II. System Design and Implementation

The system-level block diagram of APMD is shown in Fig. 1. It comprises five active subsystems, i.e., a microcontroller module, a radio module, sensor module, power module, and a cloud platform to store and display the collected data. The controller unit is responsible for monitoring the data collected by the sensors. The radio module is equipped with NB-IoT and WiFi to send data to the cloud platform. Based on the application and feasibility APMD can connect with any of these two protocols. The APMD consists of 8 sensors: four gas sensors CO, SO_2, NO_2, O_3, two PM sensors to detect $PM_{2.5}$, PM_{10}, along with temperature and humidity sensor. In the power module, a solar panel harvests the required power which is stored into a LiPo battery to supply power to the system during low light hours. The collected data is communicated to the cloud (ThingSpeak cloud platform) for storage/display. The APMD consists of a memory element to store data locally. An on-board GPS subsystem is incorporated for accurate geo-tagging. Our developed low power APMD could be used for energy sustainable pollution localization by deploying in a massive network. Fig. 2 shows a pictorial view of a large-scale network of APMD with WiFi and NB-IoT connectivity.

A. Sensor Selection

The PM sensor is used to monitor $PM_{2.5}$ and PM_{10} dust particles. Pollutants emitted from automobiles, industries, and power plants consist of SO_2 and NO. Fine particles, i.e., particles less than 2.5 μm in diameter, pose the highest health risk. Longer exposures to elevated concentrations of NO_2 may contribute to the development of asthma and respiratory infections. Ozone can aggravate lung diseases such as

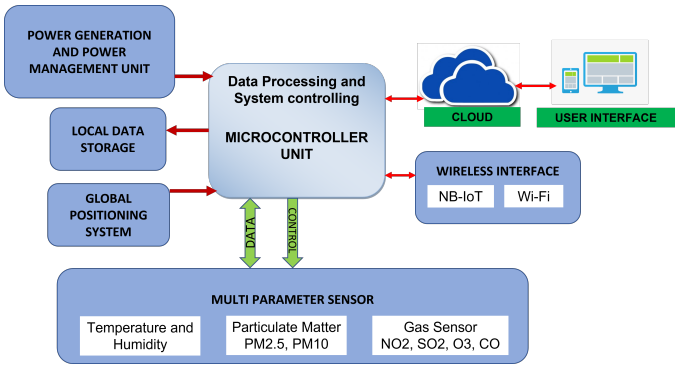

Fig. 1: Block diagram of proposed self-sustainable APMD.

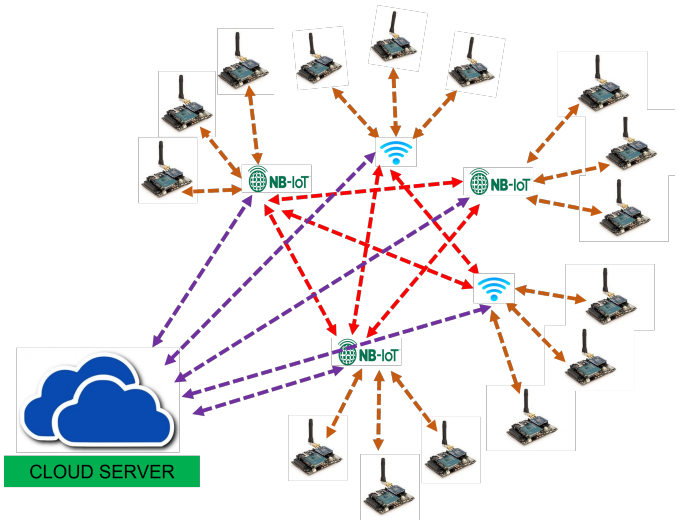

Fig. 2: Massively deployed APMD network with NB-IoT and WiFi connectivity.

asthma, emphysema, and chronic bronchitis, particularly for children, the elderly, and people of all ages who have lung diseases. SO_2 is linked to cardiovascular disease. Carbon monoxide symptoms mimic the flu: loss of consciousness, brain damage, heart irregularity, breathing difficulties, muscle weakness, abortions, and even death. Because the symptoms mimic so many illnesses, it is often misdiagnosed. Finally, the temperature and humidity sensor is also selected to monitor the comfort of people's working and living environments, as well as the impact of temperature and humidity on the parameters of the other three sensors.

B. Communication Technologies

1) NB-IoT: NB-IoT is an LPWA technology set up by 3GPP Release 16. It supports cellular data connection for low power devices in WAN. New physical layer signals and channels are designed to meet the demanding requirement of extended coverage – rural and deep indoors along with ultra-low device complexity and low-power operating modes. With an existing network gain of 20 dB, NB-IoT can increase the coverage area by 100 times. The NB-IoT communication is more suitable for low power applications compared with GPRS communication. The time-slotted synchronous protocol is optimal for Quality

of Service (QoS). Due to the trade-off between QoS and high spectrum cost, NB-IoT is preferred in applications where QoS is needed. For applications that require low latency (<10 s)and a high data rate, NB-IoT is the better choice. NB-IoT focuses mainly on the MTC class of devices that are installed at places far from the usual reach. It can be deployed by reusing and upgrading the existing cellular network but its deployments are restricted to the area supported by the cellular network [21]. The kind of IoT applications, where the duty cycle is not the limit but more frequent communication is the need, could be efficiently served by NB-IoT.

2) WiFi: IEEE 802.11 standard defines the IP based wireless technology WiFi. WiFi provides secure, reliable and high-speed communication. WiFi transmits at 2.4 GHz or 5 GHz and this enables the signal to carry more data. However, it has a trade-off between power consumption, bandwidth, and range. Typically 100 m range is common in router based WiFi deployment which is not a suitable option for IoT application that needs to be connected with massive node deployment over a large geographical area. Over a 24 hours data reporting interval, the energy consumption of WiFi is 71.4 % more than that of NB-IoT [22]. IoT application where power and range are not a constraint and a large amount of data that need to be sent to the network can have the benefit of WiFi technology, the home security system could be a good example.

III. Basic Modules of APMD

A. Power Module

The sensor mote is powered by a 0.5/3 V solar panel. Texas Instruments bq25504 energy harvester is used to harvest energy from the solar to a 5 V - 4000 mAh LiPo battery. Fig. 3 shows the system block diagram for solar energy harvester and power management design of APMD. The battery is used to power up the mote at night hours and also during the low sun-hour days. The mote operates at 3.3V. Low drop-out regulator (LDO) and DC-DC converter are used for power management purposes. The sensor node has both fixed and variable current (i.e., power) draws. The fixed draw is required regardless of whether measurements are being taken. During the measurement cycle, the current consumption of Alphasense AFE A4, Alphasense OPC N3 and DHT11 is 2.019 mA, 187 mA and 0.3 mA respectively. However, the current consumption of our designed PM sensor is 80.41 mA at 3.3V operating voltage.

B. MCU and Radio Module

The developed sensor mote utilizes an STM32L476RG microcontroller with Simcom 7020C NB-IoT radio. The microcontroller provides the embedded computation for measuring the signals from the sensors as well as implements the radio control. Five ADC channels are required for collecting the sensor data, two for each of the gas sensors, and one for the PM sensor. The temperature/humidity sensor uses the I2C protocol to transfer data. General-purpose input-output (GPIO) pins are used to control the fan and the PM sensor.

Fig. 4 shows the design of the radio module interface with the microcontroller. SIM 7020C NB-IoT module provides a

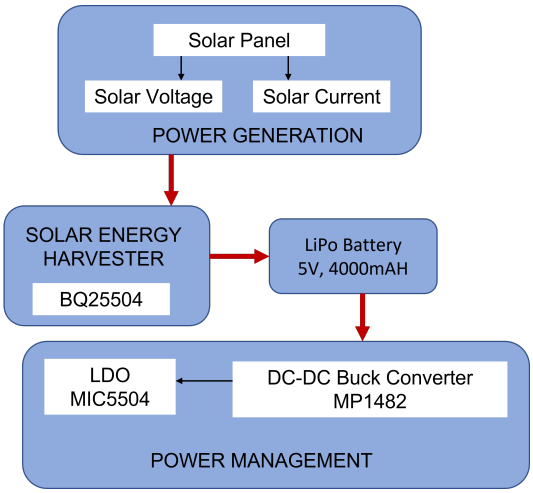

Fig. 3: Solar energy harvester and power management system with Buck converter and LDO.

1.8 V UART interface. A level translator is needed as the application is equipped with a 3.3 V UART. TXB0108PWR provided by Texas Instruments is used for this purpose. Before transmission, the data from the five sensors are grouped into a 128-bit packet and transmitted at a carrier frequency of 900 MHz. The NB-IoT module is connected to the SIM card and antenna. The SIM card, the NB-IoT module, and the antenna are core components to enable NB-IoT communications.

The system can connect the ESP8266 WiFi module with UART as a backward compatibility in case of unavailability of NB-IoT. However, WiFi is much power intensive and must have a suitable power supply (e.g., mains) while connected with the node. FGPMMOPA6H GPS module is utilized for accurate geo-tagging purpose.

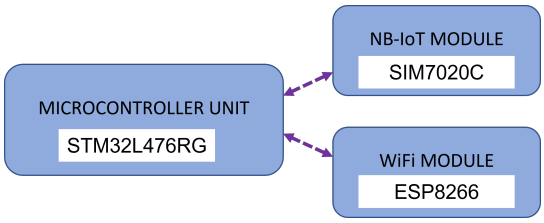

Fig. 4: NB-IoT and WiFi interface with microcontroller

C. Sensing Module

APMD is connected with an off-the-shelf Alphasense AFE-A4 gas sensor module for measuring NO_2, SO_2, CO, and O_3 [23]. During the measurement period, the power consumptions of these sensors are 1.6 mW, 1.6 mW, 1.5 mW, and 1 mW respectively while having an average response time $\leq$45 s. The APMD is also connected with DHT 11 [24] for collecting ambient temperature and humidity levels. We have designed on-board PM sensor to measure different particulate matter concentrations which is described in IV.

IV. Design of PM Sensor and its Power Control

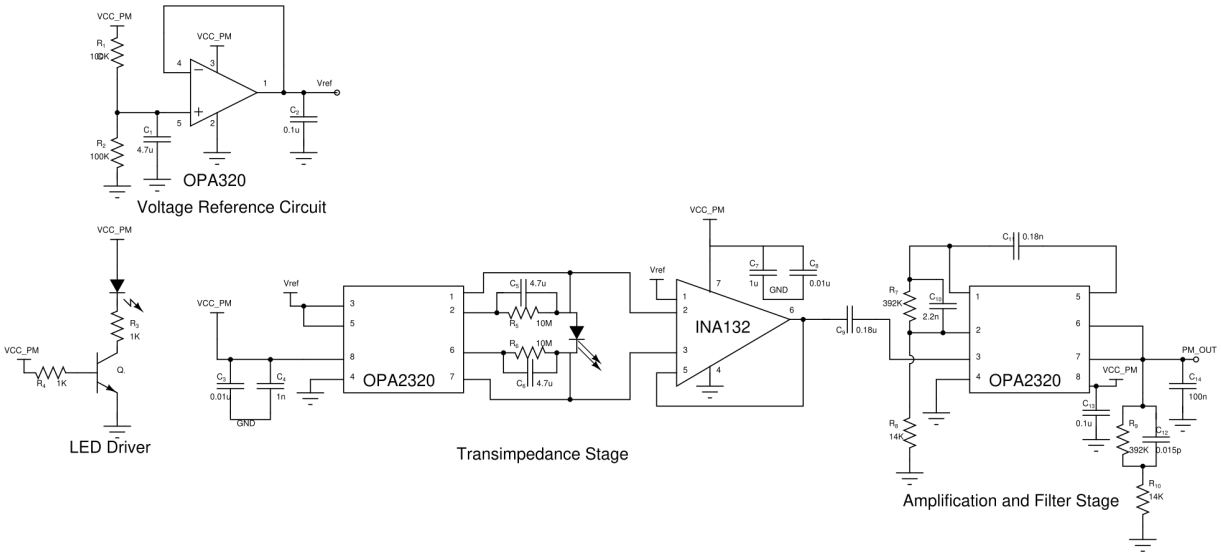

Fig. 5: PM sensor circuitry.

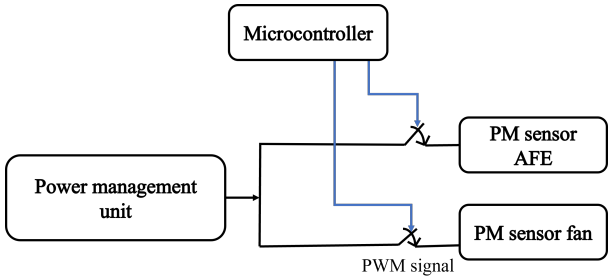

Fig. 6: Power control mechanism for PM sensor.

A. Basic PM Sensor Design

Various techniques are there to measure the suspended PM in the air. In an optical based PM measurement system, the properties of absorption and light scattering are utilized to measure different particle count, size and concentration separately. In order to optimize the cost and energy efficiency, without compromising on the quality of sensing, we chose to use a light emitting diode (LED) and a photodetector in our designed PM sensor. The PM sensor is developed using LED light scattering principle in contrast to the laser light scattering principle that the commercial PM sensors use. The basic components include a light source (LED) directed toward the particles, a photodetector to measure the light absorbed (or scattered) by the particles, an Analog Front End (AFE) to interface with the detector, and signal processing to analyze the output from the AFE. However, these instruments differ in cost, complexity, and accuracy. The designed PM sensor is able to detect particle matter with a diameter of 2.5 μm - 10 μm (PM_{10}) and diameter less than 2.5 μm ($PM_{2.5}$). The output from the photodiode is filtered and amplified to generate an output signal which is then fed to the microcontroller for further processing. To convert the photodetector output current into a voltage, the trans-impedance stage uses an OPA2320 dual package precision operational amplifier (op-amp) and an INA132 single supply difference amplifier. The filter and amplification stages use the OPA2320 op-amp with a tunable gain and basic RC filters. A light-emitting diode (LED) driver with an adjustable LED current is also included in the design. A complete design is referred in Fig. 5. The fan is a 5 V single-phase four-pole brushless dc motor with a flow rate of 1415.84 cm^3/s at a current drawn of 66 mA.

B. Power Control of On-Board PM Sensor

The PM sensor module consists of the AFE for sensing and the fan for blowing outside air inside the sensor. The fan is the most power-consuming, taking 0.33 W alone, whereas the AFE consumes only 0.079 W during the measurement period. To control the fan power consumption, we apply a PWM signal at the gate of the switch connected to fan input. When the sensor is ON, the microcontroller controls the duty cycle of the PWM signal which reduces the power consumption. The block diagram of this strategy is shown in Fig. 6. We use MOSFETs as switches for both turning ON the AFE and for providing PWM signal to the fan. We can turn on the fan using both 5 V, 66 mA or 3.3 V, 44 mA DC supply voltage. With 3.3 V at the drain and applying the PWM signal to the gate of MOSFET switch, we get 2.8 V at the source, which is connected to the power supply of the fan. Thus, the voltage drop across the switch is 0.5 V. It has been observed that the current drawn by the fan is constant at 100 ms switching period of the PWM signal. A minimum of 30% duty cycle should be applied to PWM signal. The fan is completely turned OFF for a duty cycle $D < 30\%$, which takes more than 30ms to turn ON at the next switching cycle. To avoid complete turn OFF, the duty cycle should be $\geq 30\%$. The current drawn by the fan and the respective power consumption at different duty cycles are shown in Fig. 7. The power consumption of the OPC N3 PM sensor and the onboard PM sensor are listed in Table I. A four degree polynomial fits the current profile with $R^2 = 0.999$. Similarly, the power consumption profile also can be expressed as a four degree polynomial with $R^2 = 0.999$. Thus, an optimum duty cycle can be chosen to minimize the

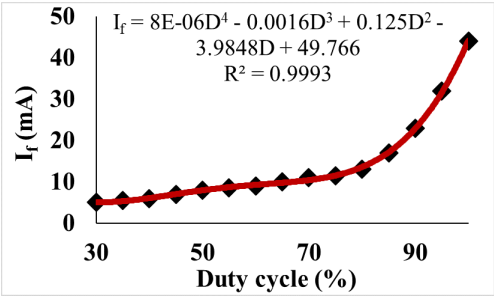

(a)

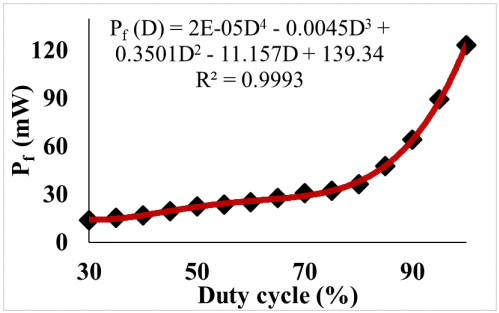

(b)

Fig. 7: (a) Current and (b) Power consumption of PM sensor fan with changing duty cycle.

TABLE I: Power consumption of on-board PM sensor

		Current (mA)	Voltage (V)	Power (W)
PM Sensor Circuit		24	3.3	0.079
PM sensor fan	Without applying PWM	66	5	0.33
	With PWM	6	2.8	0.016

power consumption of the PM sensor such that the sensor error is within the acceptable range. Estimation of optimum value of D based on the sensing error is discussed in Section VI-A.

V. Prototype Design

In this section, we discuss the design and implementation of APMD, as illustrated in Fig. 8. Specifically, in the designed system, pollution sensing, monitoring, and communication are addressed. The sensed data are collected locally as well as transmitted to an IoT cloud platform. In our design, we use the Mathworks cloud platform, named ThingSpeak. The user app is used to connect the users and application server, or request real-time data from NB-IoT devices via a cloud platform. Since it is easy to develop the user app and application server (many companies provide such a tailored development service), we focus on the technical part of the system, i.e., the design of the development board for NB-IoT devices, firmware design and implementation to enable data sensing, computing, communication, and cloud service configuration.

A. APMD Board Design

As discussed in Section III-A, the developed monitoring device consists of a solar energy harvester as a renewable source of energy and a LiPo battery as backup. The communication protocol employed is NB-IoT (5G eMTC) and/or WiFi. SIM7020C is used as an NB-IoT module in the APMD. It can work on multi-band NB-IoT and consumes extremely low power in sleep mode and idle mode. The device can operate at 2.1 V - 3.6 V. During transmission it takes 110 mA current from a 3.3 V supply at 23 dBm output power. The typical data rate of SIM7020C is 26.15 kbps. The device is capable of collecting nine air pollution parameters which include three PM sensing parameters, namely, $PM_{2.5}$, PM_{10}, four gas concentration measuring parameters: SO2, NO2, O3, CO, along with temperature and humidity. The board is also incorporated with a 512 kB EEPROM to store all the data samples in it for up to 32 hours. In 1 hour the sensors collect a total of 504 samples based on a fixed sampling rate and each sample takes 4 bytes in the memory, that can be retrieved at any time. This stationary sensor mote was deployed at different fixed points and real-time data is updated in a cloud database using the ThingSpeak cloud platform.

The PM sensor design described in Section IV, is incorporated in APMD. Fig. 8 shows the designed prototype incorporating the PM sensor on the backside of the board.

For outdoor deployment, the node is planned to be enclosed with IP67 rated case, with a solar panel placed on top of the enclosed package. The enclosure is designed to have air vents to pass air through it so that the fan of the PM sensor can draw air to take a new pollutant measurement. After the PM sensor, the air is directed towards the gas sensors and temperature/humidity sensor.

B. Data Collection Setup

As discussed in Section III, the proposed prototype is designed to monitor the environmental parameters such as temperature, humidity, PM_{10}, $PM_{2.5}$, NO_2, Ozone, CO, SO_2. Fig. 9 shows a typical data collection setup. Initially, the sensing parameters are sampled at a high sampling rate to analyze the variation profile of the signals. Let P be the total number of parameters. To find an optimum sampling interval for each parameter, the power spectral density (PSD) of that parameter is studied. If 99% of the total power is concentrated within the frequency range $\{F_{min}, F_{max}\}$, the maximum frequency of the p^{th} signal can be denoted as $F_m^p = F_{max}$. Thus, according to the Nyquist theorem, the minimum sampling frequency for the faithful reconstruction of the signal is given by, $F_s^p = 2F_m^p$. It has been observed that the sampling frequency is different for different parameters. To simplify the process, $F_{smax} = max(F_s^1, F_s^2, \ldots, F_s^P)$ is considered as the sampling frequency for all the P parameters. Hence, $T_s = \frac{1}{F_{smax}}$ is the sampling interval of all the parameters. The sensor board wakes up and collects samples from all the sensors after every T_s period, else it remains in sleep mode. Due to the slowly varying nature of the parameters, the data need not be transmitted immediately. Instead, the samples collected by the sensors are stored in the memory and transmitted after a fixed period, called *data collection interval*.

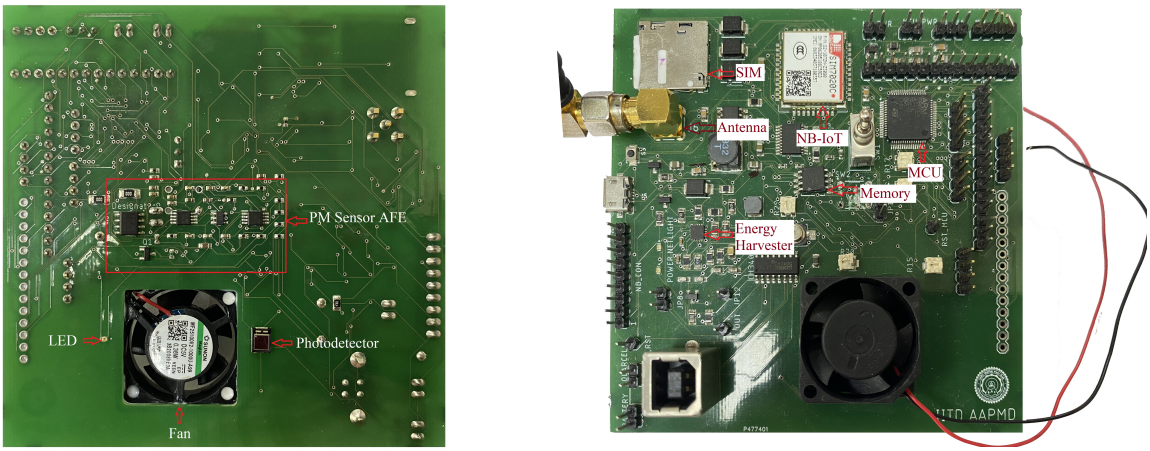

(a) Bottom side of the board

(b) Top side of the board

Fig. 8: APMD includes the STM32L476RG microcontroller, NB-IoT module, solar harvester, memory, and PM sensor.

To find an optimum data collection interval, the temporal correlation is studied for all the parameters. Let ζ^p be the time slot to find temporal correlation for p^{th} parameter, where the duration of each slot is T_s and the temporal correlation of the p^{th} parameter is above 0.9 for $\zeta^p \leq \zeta^{p*}$. Hence ζ^{p*} is the optimum data collection interval for the p^{th} parameter. Again for simplicity of the process, $L = min(\zeta^{1*}, \zeta^{2*}, \ldots, \zeta^{P*})$ is considered as the optimum data collection interval of all the P parameters. At the end of every L period, the samples stored in the memory are transmitted to the base station using the radio module of the sensor node.

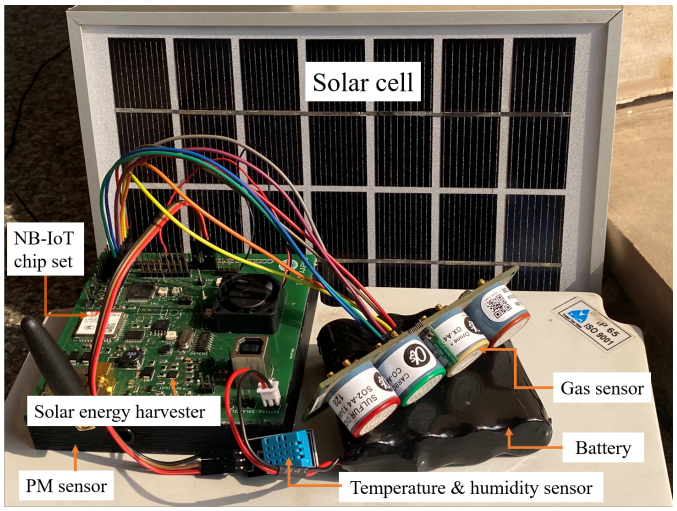

Fig. 9: Data collection setup.

The on-board PM sensor of the designed APMD is developed based on the designed circuitry provided in [25]. The sensors always introduce some errors while sensing the environment. Moreover, in the designed prototype the on-board PM sensor may have some design error. Thus, it is important to validate the efficiency of the on-board PM sensor. Since, OPC N3 PM sensor is commercially available and reliable, though high energy consuming and costly compared to the PM sensor given in [25], OPC N3 PM sensor data are considered as a reference to compare with data collected by our designed on-board PM sensor.

The on-board PM data collected from the experimental setup, shown in Fig. 9 have been stored in the cloud. It has been observed that the on-board PM data is slightly different from the actual data collected from the OPC N3 PM sensor, which infers that the on-board PM data need to be calibrated with respect to the reference data to reduce the sensing error. To calibrate the on-board PM sensor data, a polynomial regressor model is proposed in this work. Among the various machine learning models, proposed in the literature for sensor calibration, the polynomial regressor model is less complex with comparatively lower prediction error [26]. Hence, the polynomial regressor model is used to predict or calibrate the actual data from the sensed data.

C. Firmware Development

One core component in APMD is the system firmware, specifying sensor activation, sampling rate, data processing, and transmitting to the cloud platform. We have designed and implemented the firmware in the APMD using the ATMEL Studio integrated development environment (IDE).

A schematic of the system firmware flow is shown in Fig. 10. Initially, the sensors and the communication module are in power-down mode. The sensors are activated periodically to collect samples; they are turned off to reduce power consumption. The sensed data are stored in the memory. At the end of each measurement cycle L, the stored data are retrieved from the memory. The NB-IoT module is activated and the data are transmitted to the cloud. The memory is cleared to store the new samples collected at the next measurement cycle. In between two data collection periods, the microcontroller is put into deep sleep mode for T_s Sec.

NB-IoT supports two technical low-power modes, named power saving mode (PSM) and extended discontinuous reception. We use the PSM as the main power-saving mechanism in our design. By using this, NB-IoT will enter into the sleep mode in which it can be waken up by the nearby base station. Hence, in PSM mode, nearby base stations are not able to

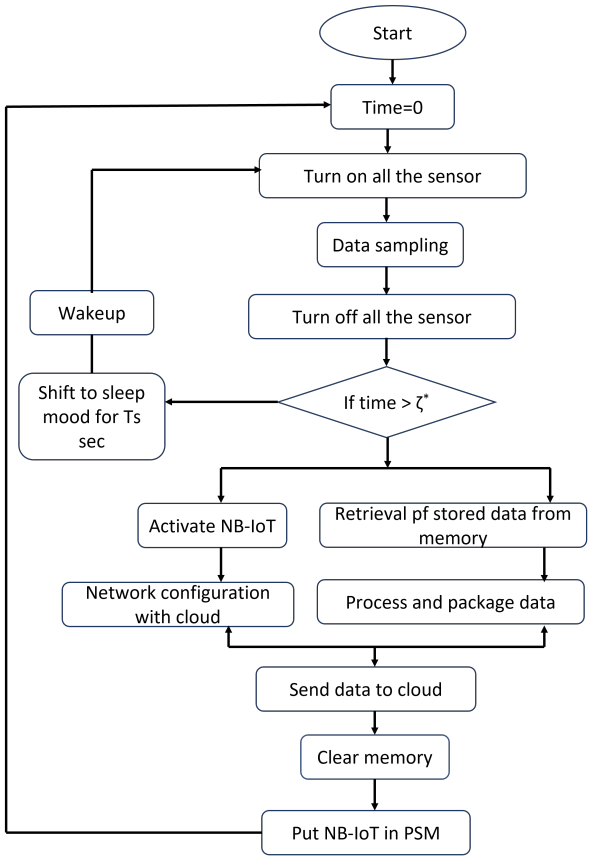

Fig. 10: Firmware flow

initialize communications with the NB-IoT device. APMD utilizing NB-IoT will be in PSM or sleep mode most of the time, hence leading to significant power saving.

VI. Results and Discussion

The experimental results of the designed APMD are discussed in this Section. To evaluate the efficacy of the designed prototype, the parameters data have been collected by using the Arduino UNO board - called as the reference setup, which is already developed and commercially available. The Arduino UNO board consists of an ATMEGA 328P microcontroller that collects samples from the sensors connected with the board and the data have been transmitted to the base station using ESP8266 WiFi module, whereas in the designed APMD the sampled data are transmitted using NB-IoT or an optional WiFi interface. As discussed in Section III, six sensors are connected with the sensor node to monitor eight parameters of the set $\mathcal{P} = \{$temperature, humidity, PM_{10}, $PM_{2.5}$, NO_2, Ozone, CO, $SO_2\}$ in the environment. In the designed APMD, the PM sensor is on-board and the other sensors are connected externally, whereas in the reference board, all sensors are connected externally and the concentration levels of PM_{10} and $PM_{2.5}$ are measured using the commercially available OPC N3 PM sensor [27]. The data collected by the development board is considered as the reference data to compare with the data collected by the designed APMD prototype.

TABLE II: Performance comparison of on-board PM sensor

		Energy consumption per sample (J)
Commercial PM sensor	Alphasense OPC-N3 (reference) [27]	28.3
	Sensirion SPS30 [29]	2.4
	Nova SDS011 [30]	3.5
On-board PM sensor	Without PWM based power control	1.636
	With PWM based power control	0.646

TABLE III: Energy saving of on-board PM sensor

		Alphasense OPC-N3	Sensirion SPS30	Nova SDS011
Energy saving of on-board sensor (%)	Without applying PWM	94.2	31	53
	With PWM	97.7	73	81.5

A. Estimation of Optimum Duty Cycle for PM Sensor

The designed PM sensor in Section IV utilizes a PWM based power control strategy as described in IV-B. On applying a PWM signal of time period 100 ms at below 30% duty cycle, the fan is unable to continue its rotation due to lesser on time compared to the off time. However, it has been observed that for $D \geq 30\%$, the fan operates continuously and the PM sensor provides valid PM data, which has been calibrated to achieve the required accuracy. The optimal duty cycle is decided based on the acceptable error (RMSE) threshold which is 1.6 and 2.7 for $PM_{2.5}$ and PM_{10}, respectively [28]. Although the sensing error increases with the decrease in duty cycle, calibrating the sensor at a particular duty cycle reduces the sensing error, which is comparable to the error achieved at 100% duty cycle. Fig. 11 shows that for both $PM_{2.5}$ and PM_{10} the obtained RMSE values for $D \in [30\%, 100\%]$ lies within the threshold. Thus, $D = 30\%$ is set as the duty cycle of the PWM signal to minimize the power consumed by the fan of the on-board PM sensor.

As shown in Table II, the on-board PM sensor consumes 0.64 J energy to collect one sample incorporating PWM duty cycle based power control mechanism, which is 60% less than without power controlled PM sensor. The power consumption of the on-board PM sensor is compared with three commercially available PM sensors, such as Alphasense OPC-N3, Sensirion SPS30, and Nova SDS011. Table II shows the performance comparison of the on-board PM sensor with the commercial PM sensors. The energy saving of on-board PM sensor with respect to the commercial sensors are listed in Table III.

B. Estimation of Optimum Parameter Values for APMD

As discussed in Section V-B, the maximum frequency of the signals is estimated from their PSD. Fig. 12 presents the PSD of the eight parameters of the set $\mathcal{P}$. The set comprising the maximum frequency of the signals is given by, $\mathcal{F}_m = \{$0.004, 0.0043, 0.008, 0.0062, 0.0054, 0.0027, 0.0056, 0.0042$\}$ Hz. Accordingly, the set comprising the Nyquist sampling frequency is given by, $\mathcal{F}_s = 2\mathcal{F}_m$. Thus, the sampling interval

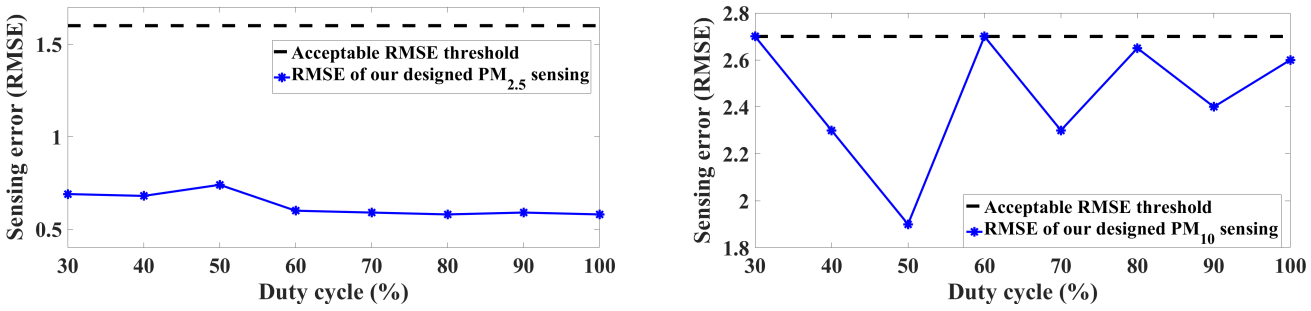

(a) $PM_{2.5}$ (b) PM_{10}

Fig. 11: RMSE versus duty cycle for $PM_{2.5}$ and PM_{10}.

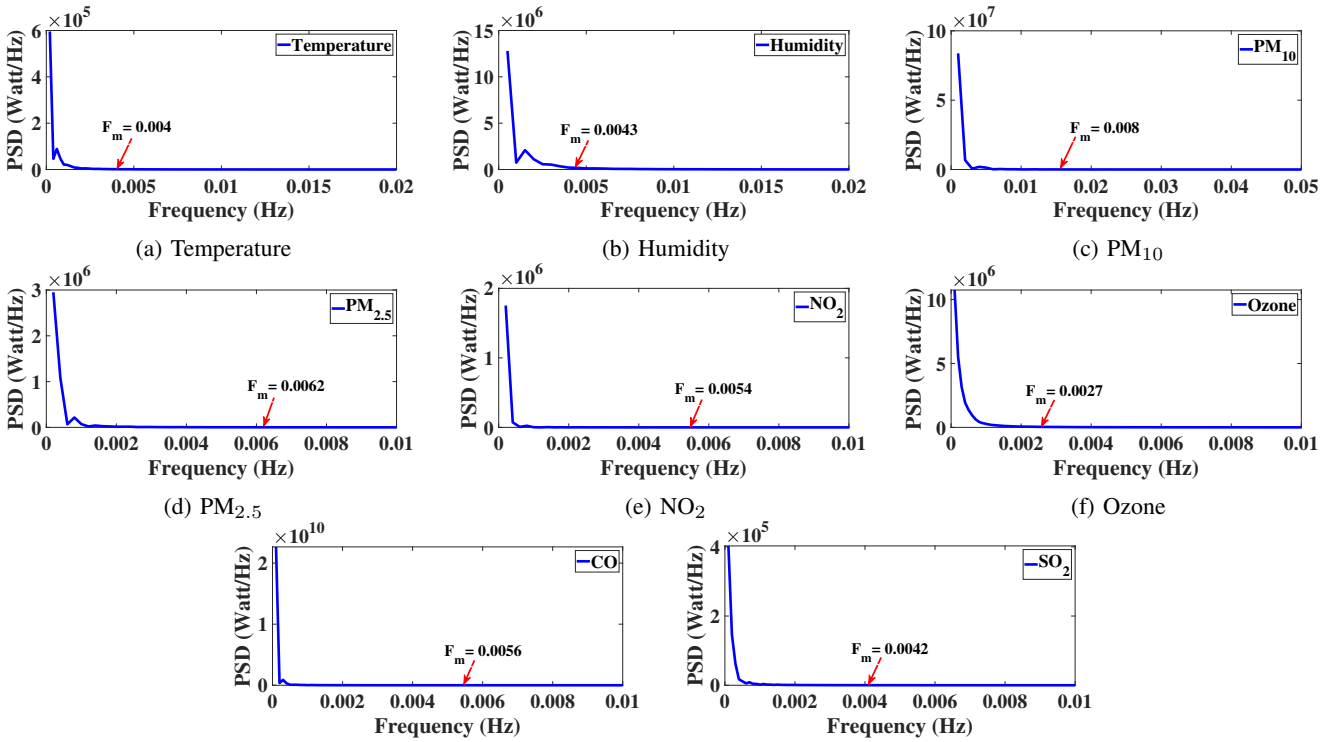

(a) Temperature (b) Humidity (c) PM_{10}

(d) $PM_{2.5}$ (e) NO_2 (f) Ozone

(g) CO (h) SO_2

Fig. 12: PSD of the sensing parameters.

of all the parameters is set as $T_s = \frac{1}{0.016} \approx 62$ s. The sensor node wakes up at every 62 s interval, collects a sample from all the sensors and stores it in the memory.

Fig. 13 presents the variation of temporal correlation with time slot ζ, where the slot duration is 62 s. Intuitively, the temporal correlation decreases with the increase in time. Hence, the data collection interval is chosen such that the data variation is small within that interval. It helps to keep track of the parameter variation and take necessary action upon exceeding the satisfactory level. Considering 0.9 as a threshold value to decide the high correlation among the data, the set comprising the optimum value of ζ^* for all the parameters is given by $\mathcal{L} = \{68, 69, 29, 37, 76, 296, 91, 66\}$. Thus, the base station data collection interval for all the parameters is set as $L = 29T_s \approx 1800$ s.

C. Energy consumption of the sensors

As discussed in Sections III and IV, the designed APMD is equipped with low power on-board PM sensor, whereas the reference setup is equipped with OPC N3 PM sensor. The accuracy of the on-board PM sensor is measured with respect to the OPC N3 PM sensor. To measure temperature and humidity, DHT11 sensor is used in both the designed APMD and reference setup. Similarly, AFE A4 gas sensors are used to measure the gas pollutants in both the designed APMD and reference setup. The energy consumption of all the sensors to collect one sample is listed in Table IV.

D. Performance Comparison of the Designed APMD and Reference Board

To evaluate the performance of the designed prototype, a comparison of sensing signals, collected by the designed

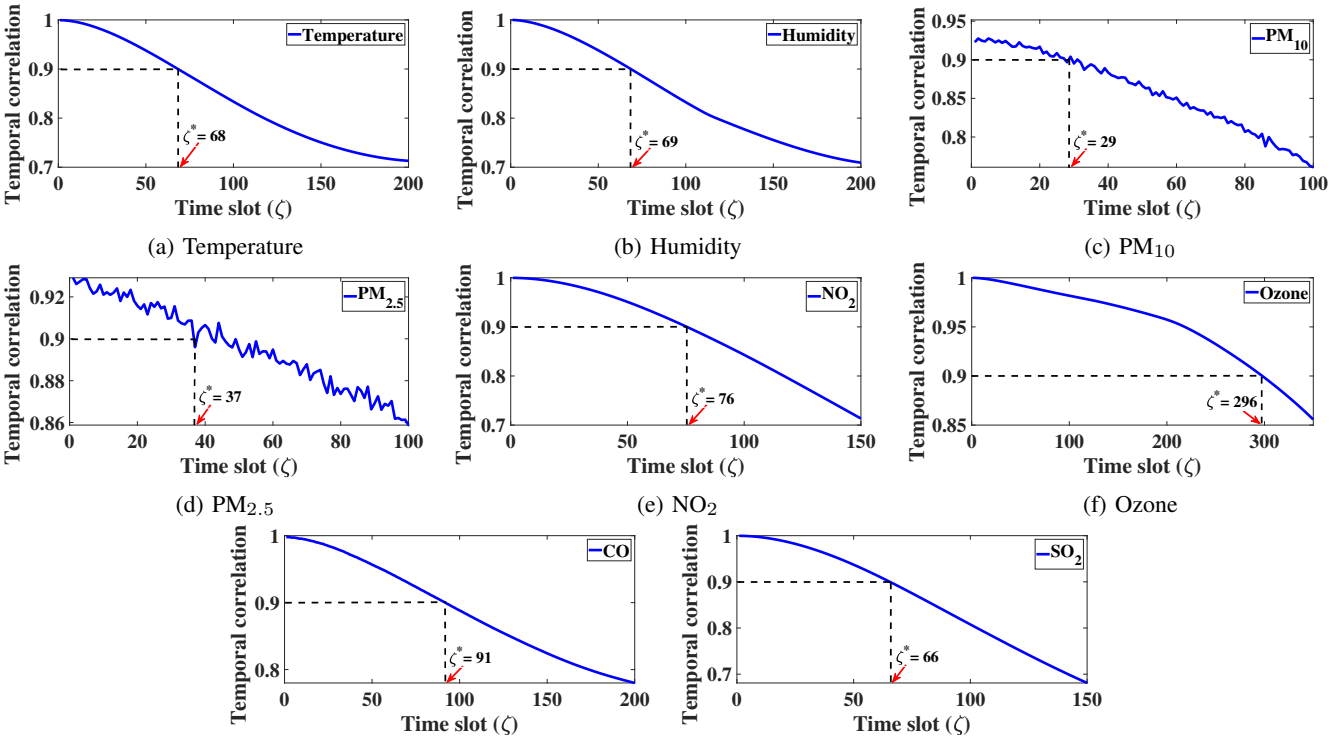

(a) Temperature (b) Humidity (c) PM_{10}

(d) $PM_{2.5}$ (e) NO_2 (f) Ozone

(g) CO (h) SO_2

Fig. 13: Temporal correlation versus ζ.

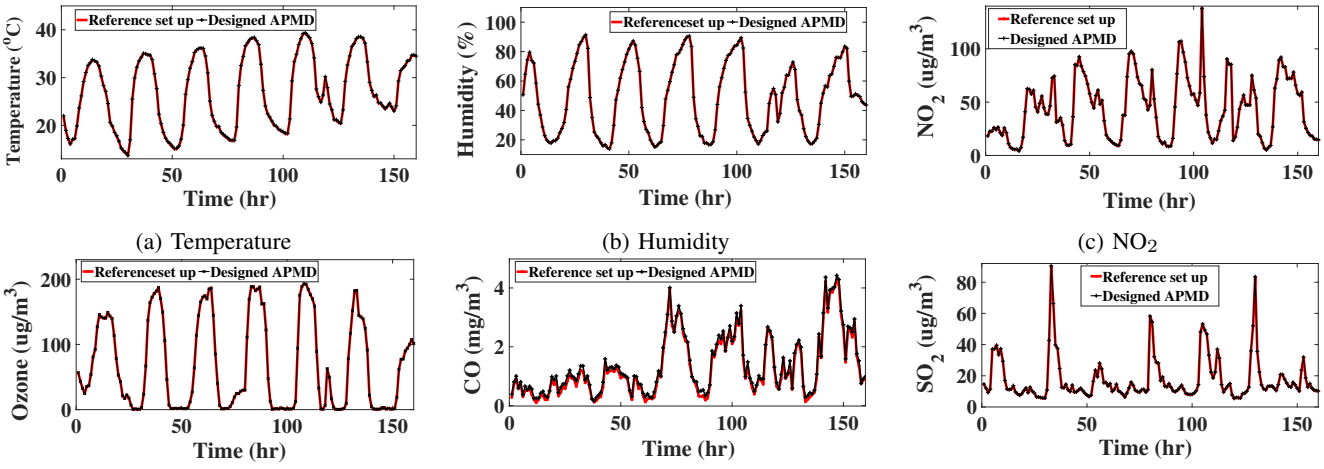

(a) Temperature (b) Humidity (c) NO_2

(d) Ozone (e) CO (f) SO_2

Fig. 14: Temperature, humidity, and gas sensors data collected by the designed APMD and reference setup.

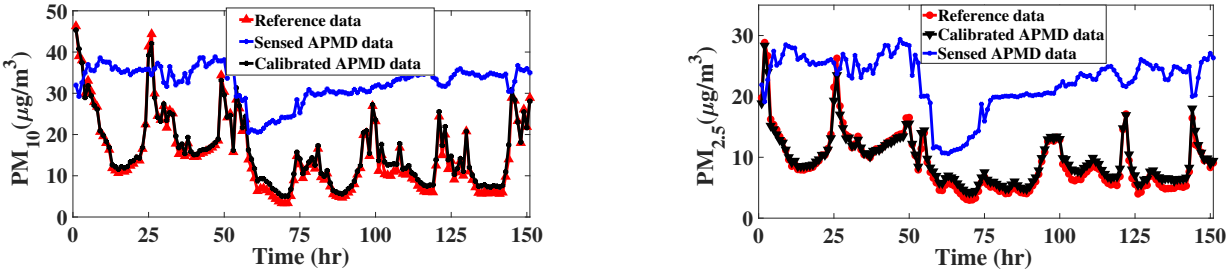

(a) PM_{10} (b) $PM_{2.5}$

Fig. 15: PM sensor data collected by the designed APMD and reference setup.

TABLE IV: Specification of the sensors

Sensors	DHT11	AFE A4 gas sensors	OPC N3 PM sensor	Designed PM sensor
Operating voltage (V)	3.3	5	5	3.3
Heat up time (sec)	2.5	1	30	2
Sensing time (sec)	1	1	1	2
Heat up current (mA)	1	5	187	68
Sensing current (mA)	1	3	50	30
Energy consumption per sample (J)	0.011	0.04	28.3	0.646

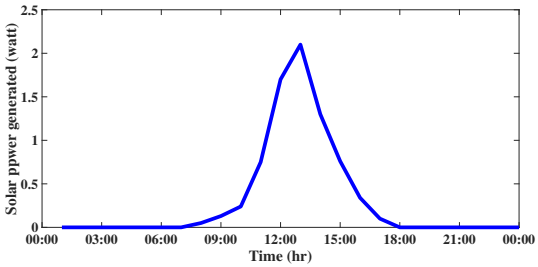

Fig. 16: Solar power generated in 24 hrs.

APMD and the collocated reference setup at the same time in the month of August 2021, is shown in this subsection. The sensing signals are reconstructed using the data collected by the reference setup and the designed APMD.

A comparison of the environmental parameters sensed using the externally connected sensors collected from the prototype and the reference setup is shown in Fig. 14. It can be observed that for each parameter the sensing signals collected from the designed APMD prototype are following the respective reference signal. The sensing error of the parameters in terms of RMSE is listed in Table VI. Similar to the study in [28], considering the RMSE $= 2.7$ as the threshold value, the sensing errors of all the signals obtained using the designed APMD are much lower than the threshold.

Two polynomial regressor models are used to predict $PM_{2.5}$ and PM_{10}. The models are trained using the initial samples of OPC N3 and the on-board PM sensors, where the input to the models are the on-board PM data and the output of the models are the reference data of the OPC N3 PM sensor. It has been observed that the prediction error is minimum if the training length lies within $220 - 250$ samples. Hence, the models are trained using 230 samples collected in 4 hrs, where the sampling interval is 62 s. Fig. 15 shows the variation of PM data collected from the OPC N3 PM sensor, the designed PM sensor, and the calibrated PM data. It can be observed that the calibrated PM data are perfectly following the actual data.

The range of sensing parameters are divided into three levels (low, medium, and high) based on the AQI, as shown in Table V. For different levels of parameters, the sensing errors are listed in Table VI. The designed APMD is equipped with low power on-board PM sensor, whereas, the reference setup is equipped with OPC N3 PM sensor. The sensing error of the on-board PM sensor is computed with respect to the OPC N3 PM sensor. To measure temperature, humidity, and the gas pollutants, DHT11 and AFE A4 gas sensors are used in both the designed APMD and reference setup. It can be observed that sensing error is slightly higher for the low AQI level of the parameters compared to the high AQI level.

From Table VI, it can be observed that the sensing errors of the PM parameters are higher than the other parameters. However, the sensing errors of $PM_{2.5}$ and PM_{10} are 0.7 and 2.7, respectively, which are lower than the threshold value. Since the externally connected sensors are the same in both the reference setup and the designed APMD setup, the average sensing error reduces to 0.44.

A comparison of energy consumption among the developed prototype and the reference setup is shown in Fig. 18. The experiment was performed in two powering modes. In the first case, each sensor node was powered by a battery. A fully charged 3.7 V, 10000 mAh Li-ion battery was connected to the node to observe the energy consumption profile. In this case, the voltage and current drawn from the battery were measured periodically when the device was active, to find the energy consumption of the node. As initially the battery is fully charged, the remaining energy can be calculated as $E_{batt}(n) = E_{batt}(n-1) - E_{con}(n)$, where $E_{batt}(n)$ is the remaining energy of the battery at the n^{th} time instant and $E_{con}(n)$ is the energy consumption of the device between $(n-1)^{th}$ and n^{th} time instants. As shown in Fig. 18(a), the battery lifetime of the reference setup is much lower than the designed APMD. Since the designed APMD is optimized for the air pollution monitoring application, the current drawn by the device is lower than that of the reference setup. The current drawn by the NB-IoT module in sleep mode is much lower than that with WiFi, the designed APMD is more energy efficient compared to the reference setup. Further, the duty cycle based power controlled PM sensor adds more to the power saving of the designed APMD.

In the second case, each sensor node was powered by a solar energy harvester along with a 3.7 V, 10000 mAh Li-ion rechargeable battery. The power generated by the solar panel has been measured hourly, which is depicted in Fig. 16. Initially, the battery was fully charged and a 9 cm$\times$12 cm solar cell was connected to the harvester to harvest energy from the ambient and recharge the battery in case of both the developed APMD and the reference setup. Since the Arduino board does not have any energy harvester, the energy harvester of the developed APMD was used to recharge the battery connected with the reference board. During the day time, the required energy is supplied by the solar cell and access energy is stored in the battery. During the night, the sensor node uses the stored energy to continue its sensing and transmission. To find the energy harvested from the solar cell, the hourly solar radiation was measured in kWh/m^2. Considering efficiency as 10%, the energy harvested E_h by the solar energy harvester is calculated. Thus, the residual energy of the battery is calculated as $E_{batt}(n) = E_{batt}(n-1) - E_{con}(n) + E_h(n)$, where $E_h(n)$ is the energy harvested between the $(n-1)^{th}$ and n^{th} time instants.

The energy consumption of the devices was calculated by

TABLE V: Different levels of air pollution monitoring parameters

Parameters	Temperature (^oC)	Humidity (%)	PM_{10} ($\mu g/m^3$)	$PM_{2.5}$ ($\mu g/m^3$)	NO_2 ($\mu g/m^3$)	Ozone ($\mu g/m^3$)	CO (mg/m^3)	SO_2 ($\mu g/m^3$)
Low pollution (AQI: $0-50$)	$0-15$	$0-30$	$0-54$	$0-12$	$0-96$	$0-102$	$0-4.8$	$0-89$
Medium pollution (AQI: $51-100$)	$15-30$	$30-60$	$54-154$	$12-35$	$96-182$	$102-133$	$4.9-10$	$89-190$
High pollution (AQI: $101-200$)	$30-45$	$60-100$	$154-354$	$35-150$	$182-1184$	$133-200$	$10.5-17$	$190-772$

TABLE VI: Sensing error of the parameters

Parameters		Temperature	Humidity	PM_{10}	$PM_{2.5}$	NO_2	Ozone	CO	SO_2
Sensing error (RMSE)	Low pollution	0.018	0.038	2.73	0.72	0.047	0.018	0.017	0.037
	Medium pollution	0.017	0.037	2.69	0.69	0.047	0.017	0.017	0.036
	High pollution	0.016	0.037	2.68	0.69	0.046	0.017	0.016	0.035
Average		0.017	0.037	2.7	0.7	0.046	0.017	0.017	0.036

TABLE VII: Performance comparison of APMD

Parameter	Oizom Polludrone [31]	APMD in [10]	Reference Board	Designed APMD
Average error (MAE)	–	38.89%	–	6.7%
Power (W)	2.5	–	0.46	0.042
Sampling interval	–	10 min	62 s	62 s

TABLE VIII: Comparison between WiFi and NB-IoT

Communication modules	WiFi (ESP8266EX) [32]	NB-IoT (SIM 7020) [33]
Operating voltage (V)	3.3	3.3
Turn on and connection setup time (s)	10	0.5
Current drawn during setup period (mA)	105	0.0035
Transmission mode current (mA)	65	110
Power save mode (mA)	NA	0.0034
Sleep mode (mA)	0.02	0.4
Data transmission rate (kbps)	4500	26

measuring the supply voltage of the battery and current drawn by the device at different time instants. The energy harvested by the solar energy harvester was computed by measuring the voltage and current of solar panel at different time instants. Since initially the battery was fully charged, the residual energy of the battery was calculated by subtracting the energy consumption of the device from the energy available in the battery and adding the harvested energy during day time. Since the decreasing residual energy gives a clear inference of lifetime of the node, it has been presented to show the comparison between our designed APMD and the reference setup. The battery voltage at different time instants was also measured for the APMD and the reference setup in both the cases (case1: without solar energy harvester and case2: with solar energy harvester), which is presented in Fig. 17. It has been observed that the voltage level slowly decays from 3.7 V to 2.5 V and then suddenly dropped to 0 V in purely battery-powered nodes, indicating that the battery circuit went to 'shut down' mode beyond a low voltage threshold. Whereas, in case of solar powered APMD, the voltage remains almost constant.

From Fig. 18(b) it can be observed that the residual energy of the battery in the reference setup decreases gradually, whereas, it is non-decreasing in the designed APMD. Hence, the battery in the reference setup needs to be recharged manually after a period, whereas the setup made using the proposed prototypes is self-sustainable.

As discussed in Section VI-B, data from all the eight sensors are transmitted to the base station after every 1800 s with 62 s sampling interval. Therefore, after every 1800 s interval about 29 samples are transmitted to the base station. As each sensing parameter takes 4 Bytes memory, one packet of eight parameters contains 7.42 kB data, which needs 0.28 s time to transmit through NB-IoT, whereas it takes 1.64 ms when using WiFi. Table VIII shows the current consumption of ESP8266 WiFi module and SIM 7020 during connection set up, transmission mode, and power saving mode. It is noted that, while turning ON, WiFi takes much longer time and consumes higher current to set up the connection. As the APMD is expected to be in sleep mode for most of the time, extremely low energy consuming power saving mode (PSM) of NB-IoT can be utilized during that time which is not available in WiFi. Accordingly, the total energy consumption of APMD for one data packet transmission using NB-IoT and WiFi are 0.305 J and 3.4 J, respectively. Hence, if the radio module is turned ON only during data transmission and kept OFF for the rest of the period, NB-IoT based communication consumes 97% less energy compared to WiFi.

Among the state-of-the-art APMDs the low cost sensor based APMD, reported in [10], has been found to be the most competitive compared to the designed APMD. Additionally, among the commercially available air pollution monitoring systems, the Oizom APMD [31] is noted to be the most competitive. Hence the designed APMD is compared with the Oizom Polludrone data. Performance comparison among the competitive APMDs and the proposed one is shown in Table VII. All the performance matrices of the designed APMD are not comparable with the APMD developed in [10] and Oizom Polludrone [31], which is due to a mismatch of used sensors and their sampling intervals. Hence, a performance

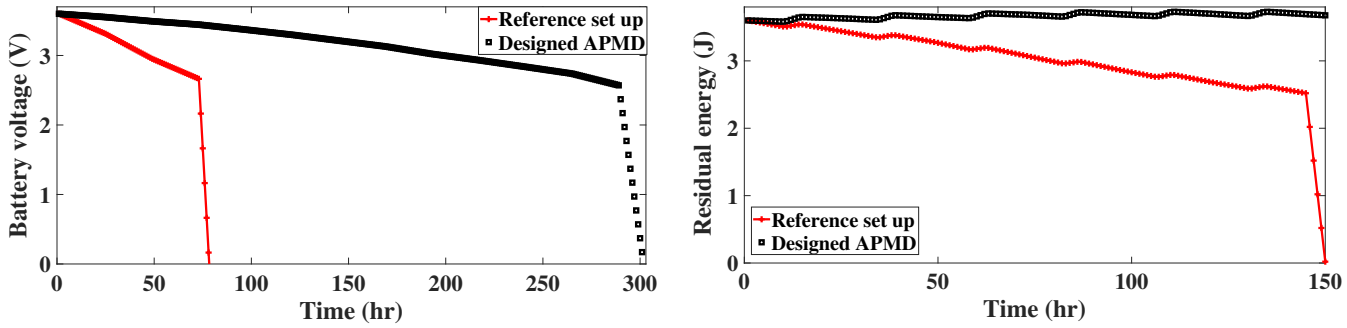

(a) Battery powered (b) Solar powered

Fig. 17: Comparison of battery charging and discharging behavior of the designed APMD and the reference setup.

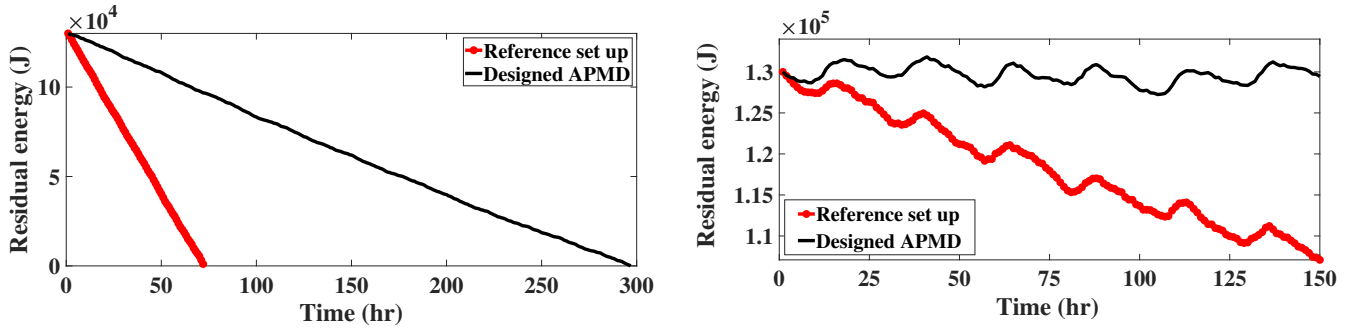

(a) Battery powered (b) Solar powered

Fig. 18: Comparison of energy consumption behavior of the designed APMD and the reference setup.

comparison among the designed APMD and the reference setup is also shown in Table VII. The sensing error is the deviation of a sensing signal, obtained using the developed prototype from their reference values, which is computed in terms of mean absolute percentage error (MAPE) to compare with [10]. The average sensing error of all the parameters is MAPE $= 6.7\%$, which demonstrates that the signal quality is not compromised. NB-IoT complaint APMD is superior in terms of power consumption and coverage range compared to the reference setup. It has been observed that, compared to the reference setup, the proposed AMPD is 90.8% more power efficient with 44 times higher coverage range. The designed APMD is 98.3% more power efficient compared to the commercial Oizom Polludrone [31].

VII. Conclusion

In this paper, we have presented a prototype design and evaluation of a low cost, portable air pollution monitoring system. The proposed APMD comprises our designed on-board PM sensor along with other off-the-shelf sensors to measure different ambient pollutants. It uses a cloud-based service to develop high resolution pollution map of a large area in real time. We have validated our designed system performance with a calibrated reference node to demonstrate that our system yields accurate estimates. The PWM based power control mechanism of the in-build PM sensor saves up to 97% power compared to the commercially available Alphasense OPC N3 PM sensor. Moreover, the developed optimized multi-sensing prototype module is 90.8% more power efficient with higher coverage range compared to the competitive reference design.

References

[1] D. Santi *et al.*, "Seasonal variation of semen parameters correlates with environmental temperature and air pollution: A big data analysis over 6 years," *Environmental Pollution*, vol. 235, pp. 806–813, 2018.

[2] L. Zhao, W. Wu, and S. Li, "Design and implementation of an IoT-based indoor air quality detector with multiple communication interfaces," *IEEE Internet Things J.*, vol. 6, pp. 9621–9632, 2019.

[3] A. Kumar, I. P. Singh, and S. K. Sud, "Indoor environment gas monitoring system based on the digital signal processor," in *Proc. International Multimedia, Signal Processing and Communication Technologies*, 2009, pp. 245–249.

[4] CISCO. Internet of things. [Online]. Available: https://www.cisco.com/c/en/us/products/collateral/se/internet-of-things/at-a-glance-c45-731471.pdf

[5] E. M. Migabo, K. D. Djouani, and A. M. Kurien, "The narrowband Internet of Things (NB-IoT) resources management performance state of art, challenges, and opportunities," *IEEE Access*, vol. 8, pp. 97 658–97 675, 2020.

[6] Y. Lin, H. Tseng, Y. Lin, and L. Chen, "NB-IoTtalk: A service platform for fast development of NB-IoT applications," *IEEE Internet Things J.*, vol. 6, no. 1, pp. 928–939, 2019.

[7] D. M. G. Preethichandra, "Design of a smart indoor air quality monitoring wireless sensor network for assisted living," in *Proc. IEEE International Instrumentation and Measurement Technology Conference*, 2013, pp. 1306–1310.

[8] S. Bhattacharya, S. Sridevi, and R. Pitchiah, "Indoor air quality monitoring using wireless sensor network," in *Proc. International Conference on Sensing Technology*, 2012, pp. 422–427.

[9] P. Zappi, E. Bales, J. H. Park, W. Griswold, and T. Š. Rosing, "The citisense air quality monitoring mobile sensor node," in *Proc. Conference on Information Processing in Sensor Networks, Beijing, China*. Citeseer, 2012, pp. 16–19.

[10] S. Ali, T. Glass, B. Parr, J. Potgieter, and F. Alam, "Low cost sensor with iot LoRaWAN connectivity and machine learning-based calibration for air pollution monitoring," *IEEE Trans. Instrum. Meas.*, vol. 70, pp. 1–11, 2020.
[11] M. Rosmiati, M. F. Rizal, F. Susanti, and G. F. Alfisyahrin, "Air pollution monitoring system using LoRa module as transceiver system," *Telkomnika*, vol. 17, no. 2, pp. 586–592, 2019.
[12] M. Rossi and P. Tosato, "Energy neutral design of an IoT system for pollution monitoring," in *Proc. IEEE Workshop on Environmental, Energy, and Structural Monitoring Systems*, 2017, pp. 1–6.
[13] K. Hu, V. Sivaraman, B. G. Luxan, and A. Rahman, "Design and evaluation of a metropolitan air pollution sensing system," *IEEE Sensors J.*, vol. 16, no. 5, pp. 1448–1459, 2015.
[14] Vanderbilt University: MAQUMON. [Online]. Available: https://www.isis.vanderbilt.edu/projects/maqumon/
[15] Fondazione ISI: Enhance environmental awareness through social information technologies (everyaware). [Online]. Available: http://www.everyaware.eu/resources/deliverables/D7.3.pdf
[16] A. Al-Ali, I. Zualkernan, and F. Aloul, "A mobile GPRS-sensors array for air pollution monitoring," *IEEE Sensors J.*, vol. 10, no. 10, pp. 1666–1671, 2010.
[17] L. Capezzuto, L. Abbamonte, S. De Vito, E. Massera, F. Formisano, G. Fattoruso, G. Di Francia, and A. Buonanno, "A maker friendly mobile and social sensing approach to urban air quality monitoring," in *Proc. IEEE Sensors Conf.*, 2014, pp. 12–16.
[18] CPCB Air Pollution in Delhi. [Online]. Available: http://cpcbenvis.nic.in/envis_newsletter/air-pollution-in-delhi.pdf
[19] S. Dhingra, R. B. Madda, A. H. Gandomi, R. Patan, and M. Daneshmand, "Internet of things mobile-air pollution monitoring system (IoT-mobair)," *IEEE Internet Things J.*, vol. 6, no. 3, pp. 5577–5584, 2019.
[20] 3GPP TR 36.824 V11.0.0, Technical Specification Group Radio Access Network, "Evolved Universal Terrestrial Radio Access (E-UTRA), LTE coverage enhancements, (Release 11)," June,2016.
[21] R. S. Sinha, Y. Wei, and S.-H. Hwang, "A survey on LPWA technology: LoRa and NB-IoT," *ICT Express*, vol. 3, no. 1, pp. 14–21, 2017.
[22] P. Das, S. Ghosh, S. Chatterjee, and S. De, "Energy harvesting-enabled 5G advanced air pollution monitoring device," in *2020 IEEE 3rd 5G World Forum (5GWF)*. IEEE, 2020, pp. 218–223.
[23] Alphasense AFE A4 Air Quality Gas Sensors. [Online]. Available: https://www.alphasense.com/wp-content/uploads/2019/10/AFE.pdf
[24] DHT11. [Online]. Available: https://www.electronicoscaldas.com/datasheet/DHT11_Aosong.pdf
[25] Texas Instruments PM2.5/PM10 particle sensor analog front-end for air quality monitoring design. [Online]. Available: https://www.ti.com/lit/ug/tidub65c/tidub65c.pdf?ts=1627496934960
[26] K. P. Murphy, *Machine Learning: A probabilistic perspective*. MIT press, 2012.
[27] Alphasense OPC-N3 particle monitor. [Online]. Available: https://www.alphasense.com/wp-content/uploads/2019/03/OPC-N3.pdf
[28] S. Chae, J. Shin, S. Kwon, S. Lee, S. Kang, and D. Lee, "PM10 and PM2.5 real-time prediction models using an interpolated convolutional neural network," *Scientific Reports*, vol. 11, no. 1, pp. 1–9, 2021.
[29] Sensirion SPS30. [Online]. Available: https://cdn.sparkfun.com/assets/2/d/2/a/6/Sensirion_SPS30_Particulate_Matter_Sensor_v0.9_D1__1_.pdf
[30] Nova SDS011. [Online]. Available: https://cdn-reichelt.de/documents/datenblatt/X200/SDS011-DATASHEET.pdf
[31] Oizom polludrone. [Online]. Available: https://oizom.com/product/polludrone-air-pollution-monitoring/
[32] ESP8266EX, Espressif Systems, Version 6.6. [Online]. Available: https://www.espressif.com/sites/default/files/documentation/0a-esp8266ex_datasheet_en.pdf
[33] SIMCOM7020X. [Online]. Available: https://www.simcom.com/product/SIM7020X.html